Journal of Statistical Physics, Vol. 62, Nos. 5/6, 1991

Hydrodynamic Interactions of Dilute Polymer Solutions in Elongational Flow

A. E. Chávez,[1] M. López de Haro,[1] and O. Manero[1]

Received November 25, 1989; final March 27, 1990

Dumbbell models are only crude representations of actual polymer molecules, but their simplicity allows for explicit calculations which in many instances have shed light on the connection between molecular properties and rheological behavior. On the other hand, hydrodynamic interactions are known to strongly influence the dynamic response of polymer solutions and this makes the representation of the hydrodynamic drag an important aspect in the calculations. In the present work, the effects of the state of flow are incorporated explicitly in the frictional properties of the FENE model of a dilute polymer solution. Results for the steady elongational viscosity and the mean square end-to-end distance are presented.

KEY WORDS: Dilute polymer solutions; dumbbell model; hydrodynamic interactions; rheological properties; elongational flows.

1. INTRODUCTION

It is rather well known that hydrodynamic interactions between macromolecules in dilute polymer solutions influence the dynamic behavior of these systems. The study of such interactions has a long history in the theory of polymer dynamics and recently has experienced a revival mostly due to the work of Ottinger.[1,2] And although the importance of the inclusion of hydrodynamic interactions in improving the predicted rheological properties arising from kinetic theoretical models has been clearly established, there still exist many open questions regarding the nature of the approximations involved in the treatment of this problem. One of the simplifications of the usual kinetic theory of bead–rod–spring models of dilute

[1] Instituto de Investigaciones en Materiales, UNAM, Coyoacán 04510, México, D.F.

0022-4715/91/0300-1255$06.50/0

polymer solutions is the notion that the average hydrodynamic drag force on a head $\mathbf{F}_i$ may be approximated by a generalized Stokes law of the form

$$\mathbf{F}_i = -\sum_j \boldsymbol{\zeta}_{ij} \cdot (\mathbf{V}_j - \boldsymbol{\beta} \cdot \mathbf{R}_j) \tag{1}$$

where $\mathbf{V}_i$ is the velocity of the ith bead, $\mathbf{R}_i$ is the position vector of the ith bead, $\boldsymbol{\beta}$ is a traceless tensor independent of position, and the friction tensors $\boldsymbol{\zeta}_{ij}$ are independent of the velocity field present in the solvent. An attempt to include explicitly the effects of the flow field in the frictional properties of a polymer solution has been carried out through the use of the consistent averaging method and the Gaussian approximation. A different approach, which deals with the hydrodynamic problem of a multibead–rod–spring chain immersed in a Newtonian solvent in steady elongational flow first and then incorporates the results into the polymer dynamics, has given elongation-rate-dependent expressions on the mobilities and friction tensors.[3]

In this paper we use these expressions, specialized to FENE dumbbells, to numerically compute approximate values for the steady elongational viscosity and the mean-square end-to-end distance as functions of the elongation rate.

The paper is organized as follows. In the next section we state the assumptions inherent in our model of the polymer solution and provide the precise forms of the steady diffusion equation and the Kramers kinetic theory expression for the stress tensor. In order to make the paper self-contained, Section 3 gives the relevant results of the mobilities obtained through the method of induced forces for the case of dumbbells. In Section 4, we introduce these expressions into the diffusion equation to derive a system of algebraic equations for the components of the tensor $\langle \mathbf{RR} \rangle$, where $\mathbf{R}$ is the relative coordinate for the dumbbell and the brackets denote a nonequilibrium average. This in turn allows us to compute the mean-square end-to-end distance and the elongational viscosity. We close the paper in Section 5 with a discussion of the results and some concluding remarks.

2. DIFFUSION MODEL FOR THE POLYMER SOLUTION

The model we adopt for the polymer solution comprises the following assumptions:

(i) There is a dilute suspension of flexible dumbbells (i.e., two identical spherical beads of radius a joined by an elastic massless connector) in a Newtonian solvent of viscosity η_S.

(ii) There is a homogeneous stationary velocity field $\mathbf{V}^0 = \boldsymbol{\beta} \cdot \mathbf{R}$, where $\boldsymbol{\beta}$ is given by

$$\boldsymbol{\beta} = \frac{\dot{\varepsilon}}{2} \begin{bmatrix} -1 & 0 & 0 \\ 0 & -1 & 0 \\ 0 & 0 & 2 \end{bmatrix} \tag{2}$$

and $\dot{\varepsilon}$ is the constant elongation rate present in the solvent in the absence of the dumbbells.

(iii) Beads represent frictional centers of resistance to the flow and move with a mean drift velocity determined by balance among systematic drag forces, potential forces, and the "entropic force" which derives from random molecular encounters (diffusion limit which suppresses explicit consideration of inertial forces).

(iv) From Eq. (1), the frictional forces $\mathbf{F}_j^H$ are related to the velocities of the beads $\mathbf{V}_i = \dot{\mathbf{R}}_i$ by

$$\mathbf{V}_i = \boldsymbol{\beta} \cdot \mathbf{R}_i - \sum_{j=1}^{2} \boldsymbol{\mu}_{ij} \cdot \mathbf{F}_j^H \tag{3}$$

where $\boldsymbol{\mu}_{ij}$ are the mobility tensors. It is in these tensors (to be given below) where the main difference with other approaches lies.

(v) The smoothed-out expression for the entropic (Brownian) force acting on bead i is

$$\mathbf{F}_i^B = -K_B T \frac{\delta \ln \Psi}{\delta \mathbf{R}_i} \qquad (i = 1, 2) \tag{4}$$

where K_B is Boltzmann's constant, T the absolute temperature, and Ψ represents the number of dumbbells that will be found within the configuration range $d\mathbf{R}_1\, d\mathbf{R}_2$ around $\mathbf{R}_1$ and $\mathbf{R}_2$.

(vi) Ψ is independent of the location of the center of mass, so that $\Psi = n\Psi_S(\mathbf{R})$, where $\mathbf{R} = \mathbf{R}_2 - \mathbf{R}_1$ is the relative coordinate and n is the (constant) number density of dumbbells.

(vii) If R_{eq} is the equilibrium length of the dumbbell, $a/R_{eq} < 1/2$, to avoid interpenetration of the beads.

(viii) Potential forces are denoted by $\mathbf{F}^c$ and for the FENE[4] dumbbell read

$$\mathbf{F}_i^c = \frac{H^1(\mathbf{R}_1 - \mathbf{R}_2)}{1 - |R_1 - R_2|^2 / R_0^2} \tag{5}$$

Under the above assumptions, the stationary distribution function obeys the diffusion equation

$$\frac{\partial}{\partial \mathbf{R}} \cdot (\beta \cdot \mathbf{R} \Psi_s) = \frac{\partial}{\partial \mathbf{R}} \cdot \left[\mathsf{D} \cdot \left(\frac{\partial \Psi_s}{\partial \mathbf{R}} + \frac{\mathbf{F}^c}{K_B T} \Psi_s \right) \right] \tag{6}$$

where $\mathsf{D} = 2K_B T(\mu_{11} - \mu_{12})$ is the diffusion tensor.

Further, since we are interested in rheological properties of the polymer solution, we need the kinetic theory expression for the stress tensor. Due to the fact that we are considering elastic connectors, it is convenient to use the Kramers form, namely

$$\tau = 2\eta_s \beta - \eta \langle \mathbf{R}\mathbf{F}^c \rangle + nK_B T \mathsf{I} \tag{7}$$

the brackets denote a stationary nonequilibrium average performed with $\Psi_s(\mathbf{R})$ (that is, the solution to the diffusion equation), i.e.,

$$\langle \mathbf{R}\mathbf{F}^c \rangle = \int d\mathbf{R}\, \mathbf{R}\mathbf{F}^c \Psi_s(\mathbf{R}) \tag{8}$$

and I is the unit tensor

3. THE METHOD OF INDUCED FORCES AND THE MOBILITY TENSORS

We now look at the hydrodynamic problem of a dilute suspensions of FENE dumbbells, assuming that the nature of the connector is such that it does not have any effect on the motion of the solvent. This is in the spirit of the Kirkwood–Riseman approach which takes the Oseen solution to the creeping flow equations.

The motion of the incompressible Newtonian solvent is assumed to obey the quasistatic Navier–Stokes equations:

$$\rho \mathbf{V}(\mathbf{R}, t) \cdot \frac{\partial \mathbf{V}(\mathbf{R}, t)}{\partial \mathbf{R}} = -\frac{\partial}{\partial \mathbf{R}} \cdot \mathsf{P}(\mathbf{R}, t) \tag{9}$$

and

$$\frac{\partial}{\partial \mathbf{R}} \cdot \mathbf{V}(\mathbf{R}, t) = 0 \tag{10}$$

for

$$|\mathbf{R} - \mathbf{R}_i| > a$$

P is the pressure tensor,

$$\mathsf{P}_{ke} = p\delta_{ke} - \eta_s \left(\frac{\partial V_e}{\partial R_k} + \frac{\partial V_k}{\partial R_e} \right),$$

p is the hydrostatic pressure, ρ the mass density of the solvent, and V_α, R_β denote the components of the solvent velocity $\mathbf{V}$ and the position vector $\mathbf{R}$.

Each bead has a (translational) velocity $\mathbf{V}_i = d\mathbf{R}_i/dt$, and obeys the equation of motion

$$m\frac{d\mathbf{V}_i(t)}{dt} = \mathbf{F}_i^H(t) + \mathbf{F}_i^{\text{ext}}(t) = -\int_{S_i(t)} \mathsf{P}(\mathbf{R}, t)\cdot \hat{N}_i\, dS + \mathbf{F}_i^{\text{ext}}(t) \tag{11}$$

S_i is the surface of bead i at time t and $\hat{N}_i$ is a unit vector normal to it pointing in the outward direction.

As boundary conditions we take $\mathbf{V}(\mathbf{R}, t) = \mathbf{V}_i(t)$ for $|\mathbf{R} - \mathbf{R}_i(t)| = a$. As was mentioned, in the absence of the dumbbell the solvent is assumed in steady elongational flow, $\mathbf{V}^0(\mathbf{R}) = \boldsymbol{\beta}\cdot\mathbf{R}$, and the pressure is $p_0 = -\frac{1}{2}\rho\mathbf{R}\cdot\boldsymbol{\beta}\cdot\boldsymbol{\beta}\cdot\mathbf{R}$.

The goal is to relate $\mathbf{F}_i^H$ to $\mathbf{V}_i$ and this is most conveniently achieved by introducing induced forces. We first set $\delta\mathbf{V} = \mathbf{V} - \mathbf{V}_0$ due to the presence of the dumbbells, substitute this in Eqs. (9) and (10), linearize the resulting equations in the perturbation $\delta\mathbf{V}$, and introduce force densities induced on the spherical beads of the dumbbells such that the fluid equations are extended to the space within the spheres. Hence, if we denote the modified pressure as $p^* = p - p_0$, the solvent equations may be cast in the form

$$\nabla\cdot\mathbf{V} = 0 \tag{12}$$

$$\rho\boldsymbol{\beta}\cdot\mathbf{V} - \eta\nabla^2\mathbf{V} = -\nabla p^* - \rho\mathbf{R}\cdot\boldsymbol{\beta}\cdot\nabla\mathbf{V} + \sum_{j=1}^{2} F_j^{\text{ind}} \tag{13}$$

where, in order to ensure that the induced forces are surface forces only, they have been defined such that

$$\mathbf{V}(\mathbf{R}, t) = \mathbf{V}_i(t) \qquad \text{for} \quad |\mathbf{R} - \mathbf{R}_i(t)| \leqslant a \tag{14}$$

$$p^* = -\rho\mathbf{R}\cdot\boldsymbol{\beta}\cdot\mathbf{V}_i \qquad \text{for} \quad |\mathbf{R} - \mathbf{R}_i(t)| < a \tag{15}$$

$$\mathbf{F}_i^{\text{ind}}(\mathbf{R}, t) \equiv \mathbf{0} \qquad \text{for} \quad |\mathbf{R} - \mathbf{R}_i(t)| > a \tag{16}$$

Further, from Eqs. (11)–(16) and using Gauss' theorem, we find

$$\mathbf{F}_i^H = -\int_{S_i(t)} \mathsf{P}(\mathbf{R}, t)\cdot\hat{N}_i\, dS$$

$$= -\int_{|\mathbf{R}\quad \mathbf{R}_i(t)|\leqslant a} \nabla\cdot\mathsf{P}\, d\mathbf{R} = \frac{4}{3}\pi\rho a^3\boldsymbol{\beta}\cdot(\mathbf{V}_i - \boldsymbol{\beta}\cdot\mathbf{R}_i)$$

$$-\int_{|\mathbf{R}\quad \mathbf{R}_i(t)|\leqslant a} \mathbf{F}_i^{\text{ind}}(\mathbf{R}, t)\, d\mathbf{R}$$

providing the necessary connection between the induced forces and the drag forces. The formal solution to Eqs. (12) and (13) allows us to eliminate the induced forces eventually and express $\mathbf{F}_i^H$ in terms of $\mathbf{V}_i$.

In the point force approximation and to lowest order in the inverse penetration length α_l, it has been shown[3] that

$$\mathbf{V}_i - \boldsymbol{\beta}\cdot\mathbf{R}_i = -\sum_{j=1}^{2} \boldsymbol{\mu}_{ij}\cdot\mathbf{F}_j^H \tag{17}$$

where

$$\boldsymbol{\mu}_{ii} = (6\pi\eta a)^{-1}\sum_{s=1}^{3}\left(1-\frac{7}{10}\alpha_s a-\frac{1}{10}\sum_{q=1}^{3}\alpha_q a\right)\hat{e}_s\hat{e}_s \tag{18}$$

$$\boldsymbol{\mu}_{ij} = (6\pi\eta a)^{-1}(\lambda_{ij}\mathbf{I}+\gamma_{ij}\hat{R}_{ij}\hat{R}_{ij}), \qquad i\neq j \tag{19}$$

$$\lambda_{ij} = \frac{3}{4}\sum_{l=1}^{3}\left[(\hat{R}_{ij}-\hat{e}_l)^2\left(\frac{7}{15}\alpha_l a-\frac{1}{2}\varepsilon_{ij}\right)+\frac{1}{2}\varepsilon_{ij}-\frac{9}{15}\alpha_l a\right] \tag{20}$$

$$\gamma_{ij} = \frac{3}{4}\sum_{l=1}^{3}\left[(\hat{R}_{ij}\cdot\hat{e}_l)^2\left(\frac{5}{2}\varepsilon_{ij}-\frac{7}{5}\alpha_l a\right)+\frac{7}{15}\alpha_l a-\frac{1}{2}\varepsilon_{ij}\right] \tag{21}$$

$\hat{R}_{ij}=\mathbf{R}_{ij}/R_{ij}$, $\varepsilon_{ij}\equiv a/R_{ij}$, $\alpha_l=(\rho\beta_e/\eta_s)^{1/2}$; β_e are the eigenvalues of $\boldsymbol{\beta}$ and $\{\hat{e}_1,\hat{e}_2,\hat{e}_3\}$ are orthonormal vectors.

4. ELONGATIONAL VISCOSITY AND MEAN-SQUARE END-TO-END DISTANCE

Now, we introduce the following dimensionless quantities:

$$R=\frac{R'}{Na},\quad t=\frac{t'}{\lambda_H},\quad \lambda_H=\frac{\xi_0(R_0)^2}{12NK_BT},\quad \varepsilon=2\lambda_H\dot{\varepsilon}',\quad \tau=\frac{\tau'}{3K_BTnN}$$

where N is the number of subunits making up the macromolecule; each subunit has length a'. The number N is thus proportional to the molecular weight and $R_0=Na'$ is the total length of the extended macromolecule. $\xi_0=6\pi\eta_s a$ is the Stokes drag on a sphere of radius a. Equations (6) and (7) are then written in the following form (after dropping the prime notation and within a hydrostatic contribution):

$$0=\frac{\partial}{\partial R}\cdot\left\{\frac{1}{3N}f(\mathbf{RR})\cdot\frac{\partial\Psi_s}{\partial\mathbf{R}}+[Hf(\mathbf{RR})\cdot\mathbf{R}-\boldsymbol{\beta}\cdot\mathbf{R}]\,\Psi_s\right\} \tag{22}$$

$$\tau=\langle H(R)\,\mathbf{RR}\rangle \tag{23}$$

where $H=1/(1-R^2)$ and $f(\mathbf{RR})=(\xi_0/2K_BT)\,\mathbf{D}$.

The dimensionless elongational viscosity is defined as

$$\bar{\eta} = -\frac{\tau_{zz} - \tau_{xx}}{\dot{\varepsilon}} \tag{24}$$

whereas the dimensionless mean-square end-to-end distance is given by $\langle R^2 \rangle$. Note that the calculation of these two quantities involves the components of $\langle \mathbf{RR} \rangle$. Multiplying Eq. (22) by $\mathbf{RR}$, averaging the resulting equation in $\mathbf{R}$ space, and using the approximations

$$\langle R_\alpha R_\beta R_\gamma R_\delta \rangle = \langle R_\alpha R_\beta \rangle \langle R_\gamma R_\delta \rangle$$
$$\langle R_\alpha^2 R_\beta^2 R_\gamma R_\delta \rangle = \langle R_\alpha^2 \rangle \langle R_\beta^2 \rangle \langle R_\gamma R_\delta \rangle$$

we arrive at the following system of nonlinear coupled algebraic equations for the components of $\langle \mathbf{RR} \rangle$.

For $\dot{\varepsilon} < 0$

$$-X_1 X_4(\langle R_x^4 \rangle + \langle R_{xy} R_{yx} \rangle + \langle R_{xz} R_{zx} \rangle) + \left(X_2 + \frac{9\alpha_1 a}{10} X_1 - \dot{\varepsilon}\right) \langle R_x^2 \rangle + \frac{2}{3N}\left(X_3 - \frac{9\alpha_1 a}{10}\right) = 0$$

$$-X_1 X_4(\langle R_y^4 \rangle + \langle R_{yx} R_{xy} \rangle + \langle R_{yz} R_{zy} \rangle) + \left(X_2 + \frac{9\alpha_1 a}{10} X_1 - \dot{\varepsilon}\right) \langle R_y^2 \rangle + \frac{2}{3N}\left(X_3 - \frac{9\alpha_1 a}{10}\right) = 0$$

$$-X_1 X_4(\langle R_z^4 \rangle + \langle R_{zx} R_{xz} \rangle + \langle R_{zy} R_{yz} \rangle) + (X_2 + 2\dot{\varepsilon}) \langle R_z^2 \rangle + \frac{1}{3N}\left(2X_3 + \frac{7}{5}\alpha_1 a \frac{\langle R_z^2 \rangle}{\langle R^2 \rangle}\right) = 0$$

$$\left[X_2 + \frac{9\alpha_1 a}{10} X_1 - X_1 X_4(\langle R_x^2 \rangle + \langle R_y^2 \rangle) - \dot{\varepsilon}\right] \langle R_{xy} \rangle - X_1 X_4 \langle R_{xz} R_{zy} \rangle = 0$$

$$\left[X_2 + \frac{9\alpha_1 a}{10} X_1 - X_1 X_4(\langle R_y^2 \rangle + \langle R_x^2 \rangle) - \dot{\varepsilon}\right] \langle R_{yx} \rangle - X_1 X_4 \langle R_{yz} R_{zx} \rangle = 0$$

$$\left[X_2 + \frac{9\alpha_1 a}{10} X_1 - X_1 X_4(\langle R_x^2 \rangle + \langle R_z^2 \rangle) + \frac{\dot{\varepsilon}}{2}\right] \langle R_{xz} \rangle - X_1 X_4 \langle R_{xy} R_{yz} \rangle = 0$$

$$\left[X_2 + \frac{7}{15}\frac{\alpha_1 a}{N\langle R^2 \rangle} - X_1 X_4(\langle R_z^2 \rangle + \langle R_x^2 \rangle) + \frac{\dot{\varepsilon}}{2}\right] \langle R_{zx} \rangle - X_1 X_4 \langle R_{zy} R_{yx} \rangle = 0$$

$$\left[X_2 + \frac{9\alpha_1 a}{10} X_1 - X_1 X_4(\langle R_y^2 \rangle + \langle R_z^2 \rangle) + \frac{\dot{\varepsilon}}{2}\right] \langle R_{yz} \rangle - X_1 X_4 \langle R_{yx} R_{xz} \rangle = 0$$

$$\left[X_2 + \frac{7\alpha_1 a}{15N\langle R^2 \rangle} - X_1 X_4(\langle R_z^2 \rangle + \langle R_y^2 \rangle) + \frac{\dot{\varepsilon}}{2}\right] \langle R_{zy} \rangle - X_1 X_4 \langle R_{zx} R_{xy} \rangle = 0 \tag{25}$$

where

$$X_1 = 2\langle H \rangle$$

$$X_2 = \frac{2}{3N}\left(X_4 + \left\{\frac{3}{4}\frac{a}{\langle R^2\rangle^{1/2}}\left(\frac{1}{\langle R^2\rangle} - 1\right) + \frac{7}{5}\alpha_1 a\left[-\frac{1}{2}\frac{\langle R_z^2\rangle}{\langle R^4\rangle} - 1 + \frac{3}{2}\left(1 - \frac{\langle R_z^2\rangle}{\langle R^2\rangle}\right)\right]\right\}\right) - X_1 X_3 \quad (26)$$

$$X_3 = 1 - \frac{3}{4}a\left\{\frac{1}{\langle R^2\rangle^{1/2}} + \alpha_1\left[\frac{7}{15}\left(1 - \frac{\langle R_z^2\rangle}{\langle R^2\rangle}\right) - \frac{6}{5}\right]\right\}$$

$$X_4 = -\frac{3}{4}a\left\{\frac{1}{\langle R^2\rangle^{1/2}} + \alpha_1\left[\frac{14}{15} - \frac{7}{5}\left(1 - \frac{\langle R_z^2\rangle}{\langle R^2\rangle}\right)\right]\right\}$$

$$\langle R^2\rangle = \langle R_x^2\rangle + \langle R_y^2\rangle + \langle R_z^2\rangle \quad (27)$$

A similar result holds for $\dot{\varepsilon} \geqslant 0$.

We have solved these systems numerically and the results for η_E/η_0 (η_0 being the zero shear-rate viscosity) and $\langle R^2\rangle/\langle R_0^2\rangle$ as functions of $\lambda_H\dot{\varepsilon}$ are shown in Figs. 1–4 for a given value of the kinematic viscosity and various values of the sphere diameter.

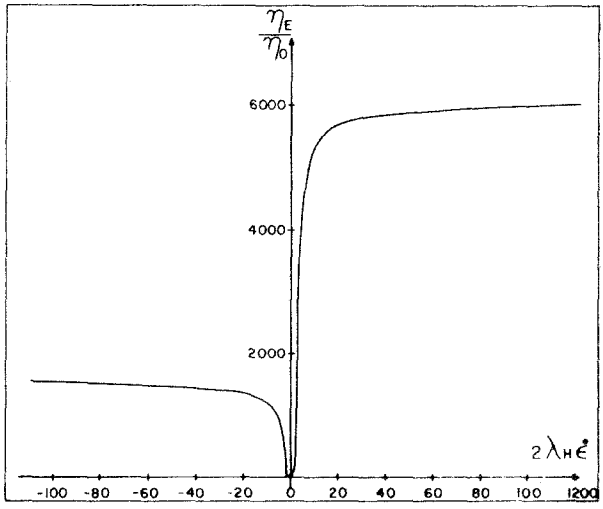

Fig. 1. Normalized extensional viscosity vs. dimensionless elongation rate for uniaxial and biaxial extensional flows. $N = 1000$.

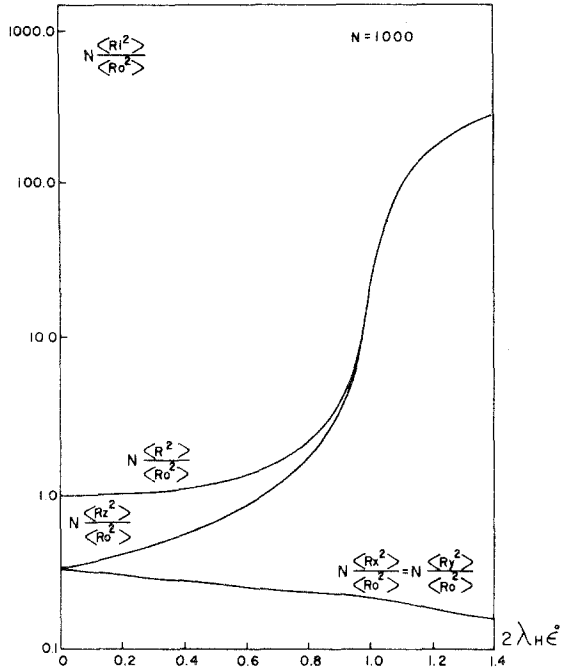

Fig. 2. Plot of $N\langle R^2\rangle/\langle R_0^2\rangle$ vs. dimensionless elongation rate for uniaxial extensional flow.

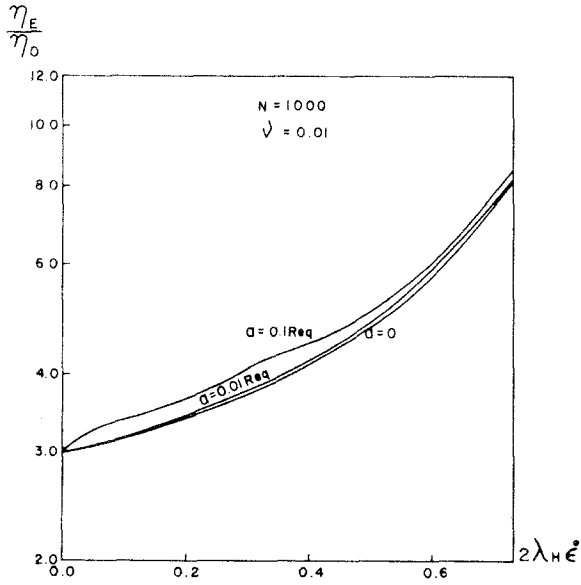

Fig. 3. Normalized extensional viscosity vs. dimensionless elongation rate. Kinematic viscosity of the solvent $\nu = 0.01$. Here $\dot{\epsilon} > 0$.

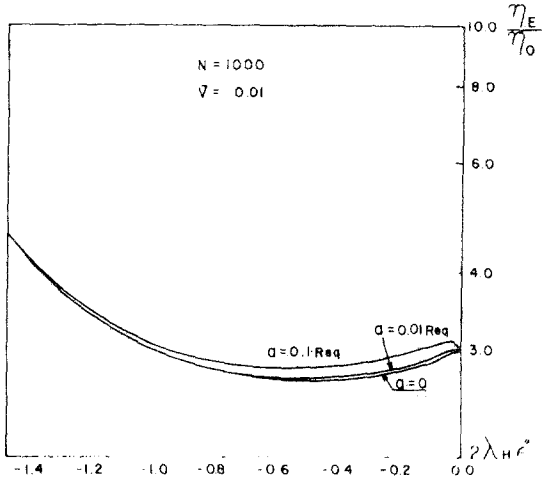

Fig. 4. Same as in Fig. 3, for $\dot{\varepsilon} < 0$.

5. DISCUSSION

For $a = 0$ (no hydrodynamic interaction), we have verified that our numerical computations comply with the limits[4]

$$\lim_{\dot{\varepsilon} \to 0} \eta_E = 3\eta_0, \qquad \eta_0 = \eta_s + nK_B T\lambda_H \tag{28}$$

$$\lim_{\dot{\varepsilon} \to \infty} \eta_E = 3\eta_s + 2nK_B T\lambda_H b, \qquad b = 3N \tag{29}$$

$$\lim_{\dot{\varepsilon} \to -\infty} \eta_E = 3\eta_s + \tfrac{1}{2}nK_B T\lambda_H b \tag{30}$$

This is depicted in Fig. 1, thus giving support to our numerical algorithm.

In Fig. 2 we show results for the moments at low elongation rates, in uniaxial extension and $a = 0$. The growth of $\langle R^2 \rangle$ is mainly due to $\langle R_z^2 \rangle$ in the vicinity of $2\lambda_H \dot{\varepsilon} = 1$. In contrast, in biaxial extensional flow (not shown), $\langle R_x^2 \rangle$ and $\langle R_y^2 \rangle$ are the mayor contributions to molecular extension, whereas the $\langle R_z^2 \rangle$ contribution is negligible for $-\lambda_H \dot{\varepsilon} = 1$. By varying the sphere radius a, we found an increase in the values of the moments of about 5% for $a = 0.1R_{eq}$, where $R_{eq} = (N+1)^{-1/2}$, around the vicinity of $\lambda_H \dot{\varepsilon} = 0.5$. This is not shown in Fig. 2 due to the scale used in plotting the results. However, a substantial increase was found for values within the

range $0.1R_{eq} \leqq a < 0.5R_{eq}$, and this is due to hydrodynamic interactions when the spheres come closer to each other.

The influence of sphere radius on elongational viscosity, for small $|\dot{\varepsilon}|$, is shown in Figs. 3 and 4. Radii used as parameters correspond to $a = 0$, $a = 0.01R_{eq}$, and $a = 0.1R_{eq}$. This is consistent with the fact that we have only considered the lowest order in the $\dot{\varepsilon}$ dependence of the mobilities, and is reflected in the range covered in Figs. 3 and 4.

A striking result arises by comparing the behavior of the elongational viscosities for positive and negative values of $\dot{\varepsilon}$. In uniaxial flow η_E is always an increasing function of $\dot{\varepsilon}$, whereas in biaxial flow there exists a region where η_E does the opposite (see Figs. 3 and 4). Indeed, in Fig. 4 our results show a region of strain thinning at low elongation rates that follows a small maximum when $-\dot{\varepsilon} \to 0$. The presence of this maximum and the inflection points shown in these figures reflect the mathematical complexity of the system of equations (25)–(27). Indeed, the order of the moment equations and their couplings produce a highly nonlinear system which induces this particular behavior not found in previous work.[5-7]

Another important result is that our computations did not show evidence for the presence of a hysteresis loop at low elongation rates in accordance with the predictions of Wiest *et al.*[5]

Comparison of our numerical values with those from ref. 6 shows that in the limit of low elongation rates the elongational viscosity shows a sizeable dependence on the sphere radius for both approaches. However, departures up to 20% in the numerical values are observed, which show the differences between Öttinger's method and the induced-forces approach presented here.

Finally, we should mention that, in principle, the approach recently proposed by Rabín *et al.*[8] to deal with the calculation of the full dynamic Oseen tensor in simple shear and elongational flows could also be used to examine the rheological behavior of polymer solutions. However, apart from the fact that their expressions for the mobilities look far more complicated than ours, it is not clear how their method could be extended beyond the pointlike sources of frictional force approximation, in contrast with the systematic treatment allowed by the method of induced forces used here.

REFERENCES

1. H. C. Öttinger, *J. Non-Newtonian Fluid Mech.* **33**:53–93 (1989), and references therein.
2. H. C. Öttinger, *Colloid Polym. Sci.* **267**:1–8 (1989).
3. M. López de Haro, A. Pérez-Madrid, and J. M. Rubí, *J. Chem. Phys.* **88**(12):7964–7969 (1988).

4. R. B. Bird, C. F. Curtiss, R. C. Armstrong, and O. Hassager, *Dynamics of Polymeric Liquids*, Vol. 2 (Wiley, New York, 1977).
5. J. M. Wiest, L. E. Wedgewood, and R. B. Bird, *J. Chem. Phys.* **90**(1):587–594 (1989).
6. P. Biller, H. C. Öttinger, and F. Petruccione, *J. Chem. Phys.* **85**(3):1672–1675 (1986).
7. R. B. Bird, P. J. Dotson, and N. L. Johnson, *J. Non-Newtonian Fluid Mech.* **7**:213–235 (1980).
8. Y. Rabín, S. Q. Wang, and D. B. Creamer, *J. Chem. Phys.* **90**(1):570–574 (1989).